Available online at www.sciencedirect.com
SCIENCE DIRECT®
Journal of Solid State Chemistry 173 (2003) 69–77
JOURNAL OF SOLID STATE CHEMISTRY
http://elsevier.com/locate/jssc

Structural and vibrational studies of $Li[K_x(NH_4)_{1-x}]SO_4$ and $Li_2KNH_4(SO_4)_2$ mixed crystals

Jorge Mata, Xavier Solans,* and Judit Molera

Departament de Cristal·lografia, Universitat de Barcelona, Martin i Franquès s/n, E-08028 Barcelona, Spain

Received 8 October 2002; received in revised form 13 January 2003; accepted 20 January 2003

Abstract

Mixed crystals of $Li[K_x(NH_4)_{1-x}]SO_4$ have been obtained by evaporation from aqueous solution at 313 K using different molar ratios of mixtures of $LiKSO_4$ and $LiNH_4SO_4$. The crystals were characterized by Raman scattering and single-crystal and powder X-ray diffraction. Two types of compound were obtained: $Li[K_x(NH_4)_{1-x}]SO_4$ with $x \geqslant 0.94$ and $Li_2KNH_4(SO_4)_2$. Different phases of $Li[K_x(NH_4)_{1-x}]SO_4$ were yielded according to the molar ratio used in the preparation. The first phase is isostructural to the room-temperature phase of $LiKSO_4$. The second phase is the enantiomorph of the first, which is not observed in pure $LiKSO_4$, and the last is a disordered phase, which was also observed in $LiKSO_4$, and can be assumed as a mixture of domains of two preceding phases. In the second type of compound with formula $Li_2KNH_4(SO_4)_2$, the room-temperature phase is hexagonal, symmetry space group $P6_3$ with cell-volume nine times that of $LiKSO_4$. In this phase, some cavities are occupied by K^+ ions only, and others are occupied by either K^+ or NH_4^+ at random. Thermal analyses of both types of compounds were performed by DSC, ATD, TG and powder X-ray diffraction. The phase transition temperatures for $Li[K_x(NH_4)_{1-x}]SO_4$ $x \geqslant 0.94$ were affected by the random presence of the ammonium ion in this disordered system. The high-temperature phase of $Li_2KNH_4(SO_4)_2$ is also hexagonal, space group $P6_3/mmc$ with the cell a-parameter double that of $LiKSO_4$. The phase transition is at 471.9 K.
© 2003 Elsevier Science (USA). All rights reserved.

Keywords: Phase transition; Ferroelectric material; X-ray diffraction; Raman scattering; Thermal analysis; Crystal structure; Mixed crystals; Lithium sulfate compounds; Ammonium; Potassium

1. Introduction

A great number of studies have examined the physical properties of, and phase transitions in, lithium potassium sulfate [1–4], $LiKSO_4$, and lithium ammonium sulfate [5,6], $LiNH_4SO_4$. Interest in the former is due to its pyroelectric, ionic conductivity, ferroelastic and ferroelectric properties, while interest in the latter is due to its ferroelastic and ferroelectric properties.

$LiKSO_4$ has a hexagonal structure derived from tridymite. The framework of corner-sharing LiO_4 and SO_4 tetrahedra forms cavities which are filled by K^+ ions. The framework is relatively flexible, as shown by the large number of phases in the range 123–1000 K. $LiNH_4SO_4$ is pseudo-isostructural to $LiKSO_4$ and also shows several phases. The main difference between the two structures is in the orientation of LiO_4 and SO_4 tetrahedra. All SO_4 tetrahedra have the same orientation in $LiKSO_4$. The relationship between up and down along the pseudo-trigonal axis is 1:1 in $LiNH_4SO_4$. This explains the different spontaneous polarization of the two compounds at room temperature, which is parallel to the trigonal axis in the $LiKSO_4$ and normal to the pseudo-trigonal axis in $LiNH_4SO_4$.

The S–O bond lengths are in the range 1.467(4)–1.519(4) Å in the structure of $LiNH_4SO_4$ [5] at room temperature. This is due to NH_4–O hydrogen bonds. In the structure of the $LiKSO_4$ at room temperature, the four S–O distances are equal (range: 1.464(3)–1.465(6) Å). We conclude that the dipolar contribution to the spontaneous polarization is higher in $LiNH_4SO_4$ than in $LiKSO_4$. In $LiKSO_4$ the spontaneous polarization disappears when the temperature rises and a mirror plane then appears perpendicular to the polarization axis. At room temperature the highest deviation of the ionic centers from this mirror plane is 0.30 Å (in the Li atom) in $LiNH_4SO_4$ and 2.53 Å (in K) in $LiKSO_4$. We

*Corresponding author. Fax: +34-934021340.
E-mail address: xavier@geo.ub.es (X. Solans).

0022-4596/03/$ - see front matter © 2003 Elsevier Science (USA). All rights reserved.
doi:10.1016/S0022-4596(03)00092-6

conclude that the ionic contribution to the polarization is higher in $LiKSO_4$ than in $LiNH_4SO_4$. These differences in the structural behavior of NH_4^+ and K^+, which modified the results of spontaneous polarization, also altered the results of no-lineal optics (NLO) [7,8].

The main purposes of this study are: (a) to examine the effect of the random presence of electronically different cations of similar size on the phase transition sequence of the pure compounds. (b) To study the influence of this random presence of cations on the compounds' physical properties and to search for new phases produced by new arrangements of the various cations.

A Raman scattering study of $LiK_{0.96}(NH_4)_{0.04}SO_4$ [9] and Raman and birefringence studies of $LiK_{1-x}Rb_xSO_4$ [10] preceded the work described here.

2. Experimental section

2.1. Synthesis

Lithium potassium sulfate and lithium ammonium sulfate were prepared as indicated elsewhere [1,5]. Mixtures of these compounds in several molar ratios were dissolved in water. Crystals were obtained by slow evaporation at constant temperature of 313 K. The compounds obtained were analyzed by induced condensed plasma (ICP) with a Jobin-Yvon analyzer, powder and single-crystal diffraction.

2.2. Raman scattering

Polarized Raman spectra were excited on the powder sample using a Jobin-Yvon T64000 spectrometer and argon-ion laser excitation. The detector was a Control Data CDC. The spectra were recorded with three monochromator gratings and the 514.5 nm line was used with a light power of 1.05 W. The range measured was 40–2000 cm^{-1}. All spectra were calibrated against selected neon lines. A Mettler FP84 sample warming cell was used in order to measure the spectra at 298, 423, 473, 513, 473, 423 and 298 K. The position, half-width and relative intensity of each peak were determined, assuming a Lorentzian function (the Gaussian contribution was negligible).

2.3. X-ray structure determination

The same method was followed in all single-crystal structure determinations. The intensities were collected at 298 K on an Enraf-Nonius CAD4 automated diffractometer equipped with a graphite monochromator. The $\omega - 2\theta$ scan technique was used to record the intensities. Scan widths were calculated as $A + B\tan\theta$, where A is estimated from the mosaicity of the crystal and B allows for the increase in peak width due to Mo$K\alpha_1$–$K\alpha_2$ splitting.

Details of structure determination are listed in Table 1. The unit-cell parameters were obtained by a least-squares fit to the automatically centered settings from 25 reflections ($12^\circ < 2\theta < 21^\circ$). The intensities from three control reflections for each measurement showed no significant fluctuation during data collection.

The structures were solved by direct methods, using the SHELXS-97 computer program [11] and refined by the full-matrix least-squares method, using the SHELXL-97 computer program [12]. The function minimized was $w||F_o|^2 - |F_c|^2|^2$, where the weighting scheme was $w = [\sigma^2(I) + (k_1P)^2 + k_2P]^{-1}$ and $P = (|F_o|^2 + 2|F_c|^2)/3$. The values of k_1 and k_2 were also refined. The chirality of the structure was defined from the Flack coefficient [13].

2.4. X-ray powder diffraction

Powder-diffraction data were collected with a Siemens D500 at different temperature, using Cu$K\alpha$ radiation and a secondary monochromator. The experiments were: warming from 298 to 950 K followed by cooling between the same temperatures, using an HTK Aaton Par Camera for $LiK_x(NH_4)_{1-x}SO_4$. Cooling from 298 to 150 K followed by warming between the same temperatures, using a TTK Aaton Camera for the same compound and warming from 298 to 523 K followed by cooling for $Li_2KNH_4(SO_4)_2$. The cooling and warming rates were 5 K/min and the sample was left for 10 min at measuring temperature in order to stabilize the equipment and the sample. The step size was 0.05°, the time of each step 10 s and the 2θ range was 10–80°. Cell parameters from powder diffraction were determined using 25 peaks with the TREOR97 program and refined with the WINPLOTR program [14].

2.5. Thermal analysis

The thermal analyses above room temperature were carried out in a differential thermal analysis (DTA) and thermogravimetry (TG) NETZSCH STA409. Loss of mass was not observed in the analysis of the phase transitions. The thermal analyses for temperatures below room temperature were carried out in a differential scanning calorimeter (DSC) Perkin-Elmer DSC-7. Different warming and cooling rates were used, but the results are given at 5 K/min. The weight of samples was about 80 mg and the reference material was alumina.

3. Results and discussion

The phase diagram of the binary system $LiKSO_4$–$LiNH_4SO_4$ cannot be determined from liquidus because

Table 1
Crystal data and structure refinement for different phases of $LiK_x(NH_4)_{1-x}SO_4$ measured at 298 K

	Phase III	Phase III′	Phase IV	Phase II
Formulae	$LiK_{0.97}(NH_4)_{0.03}SO_4$	$LiK_{0.97}(NH_4)_{0.03}SO_4$	$LiK_{0.93}(NH_4)_{0.07}SO_4$	$Li_2KNH_4(SO_4)_2$
Wavelength (Å)	0.71069	0.71069	0.71069	0.71069
Crystal system	Hexagonal	Hexagonal	Hexagonal	Hexagonal
Space group	$P6_3$	$P6_3$	$P6_3mc$	$P6_3$
a (Å)	5.1370(8)	5.1412(13)	5.152(2)	18.1780(14)
c	8.638(7)	8.644(8)	8.642(3)	8.595(15)
Volume (Å^3)	197.41(17)	197.9(2)	198.65(13)	2460(5)
Z, calculated density (Mg/m^3)	2, 2.368	2, 2.387	2, 2.340	12, 2.088
μ (mm^{-1})	1.669	1.687	1.622	1.142
Crystal size (mm)	$0.1\times0.1\times0.1$	$0.20.2\times0.2$	$0.1\times0.1\times0.1$	$0.1\times0.1\times0.3$
Θ range for data collection (°)	4.58–29.96	4.58–29.94	4.57–29.99	2.24–29.98
Index ranges	$-7\leqslant h\leqslant6$	$-7\leqslant h\leqslant6$	$-7\leqslant h\leqslant7$	$-21\leqslant h\leqslant0$
	$0\leqslant k\leqslant7$	$-2\leqslant k\leqslant7$	$-7\leqslant k\leqslant7$	$0\leqslant k\leqslant25$
	$-3\leqslant l\leqslant12$	$0\leqslant l\leqslant12$	$-2\leqslant l\leqslant12$	$0\leqslant l\leqslant12$
Reflections collected/unique	660/208	661/207	1026/131	2567/2421
R(int)	0.0256	0.0329	0.0153	0.0246
Completeness to $2\Theta=29.96°$	100.0%	100.0%	94.9%	95.2%
Data/parameters	208/24	207/24	131/24	2421/256
Goodness-of-fit on F^2	1.119	1.102	1.131	1.043
R_1 index (all data)	0.0271	0.0221	0.0170	0.0407
wR_2 index (all data)	0.0657	0.0498	0.0417	0.1115
Absolute structure parameter	0.12(10)	0.08(7)	0.09(16)	0.00(9)
Largest diffraction peak (e Å^{-3})	0.358	0.377	0.177	0.763
Largest diffraction hole (e Å^{-3})	−0.655	−0.280	−0.216	−0.368

Table 2
Majority phase obtained from the crystallization in water solution vs. the starting molar ratio of $LiKSO_4$ and $LiNH_4SO_4$

Molar ratio $LiKSO_4$:$LiNH_4SO_4$	Obtained phase	
Pure $LiKSO_4$		
9:1	III–$LiK_x(NH_4)_{1-x}SO_4$	$x\geqslant0.94$
7:3	III′—$LiK_x(NH_4)_{1-x}SO_4$	$x\geqslant0.94$
1:1	IV—$LiK_x(NH_4)_{1-x}SO_4$	$x\geqslant0.94$
3:7	III—$LiK_x(NH_4)_{1-x}SO_4$	$x\geqslant0.94$
1:9	$Li_2KNH_4(SO_4)_2$	
1:18	$LiNH_4SO_4$	
Pure $LiNH_4SO_4$		

$LiNH_4SO_4$ decomposes at 601 K. [5] The results, obtained from the 32 crystallization using different molar ratios of mixtures of $LiKSO_4$ and $LiNH_4SO_4$, are summarized in Table 2. The x values obtained for $LiK_x(NH_4)_{1-x}SO_4$ were in the range $1>x\geqslant0.94$. From Table 2 it is deduced that the crystals obtained are rich in potassium. This is because the solubility of the $LiKSO_4$ in water is lower than that of $LiNH_4SO_4$. The $LiK_x(NH_4)_{1-x}SO_4$ ($x\geqslant0.94$) and $Li_2KNH_4(SO_4)_2$ crystals were easy to distinguish optically since the former are equidimensional, showing the crystal forms {001} and {101} and the latter are prisms with the forms {011} and {110}. The largest crystals obtained were $2\times2\times2$ cm for $LiK_x(NH_4)_{1-x}SO_4$ ($x\geqslant0.94$) and $4\times1\times1$ cm for $Li_2KNH_4(SO_4)_2$.

Table 3
Atomic coordinates ($\times10^4$) and equivalent isotropic displacement parameters (Å$^2\times10^3$) for $LiK_x(NH_4)_{1-x}SO_4$. U(eq) is defined as one-third of the trace of the orthogonalized U_{ij} tensor

	x	y	z	U(eq)
Phase III				
S	6667	3333	4239(2)	14(1)
X	10,000	0	6297(1)	23(1)
O(1)	6667	3333	5942(10)	47(2)
O(2)	9418(6)	5977(6)	3706(5)	32(1)
Li	6667	3333	8152(13)	14(2)
Phase III′				
S	6667	3333	4242(1)	14(1)
X	10,000	0	6299(1)	23(1)
O(1)	6667	3333	5937(6)	46(1)
O(2)	9419(5)	3442(5)	3712(4)	33(1)
Li	6667	3333	8137(10)	16(2)
Phase IV				
S	6667	3333	4251(3)	14(1)
X	10,000	0	6316(3)	23(1)
O(1)	6667	3333	5957(15)	47(3)
O(2)	9430(16)	5979(18)	3701(9)	32(2)
Li	6667	3333	8160(2)	21(4)

$X=K$ and (NH_4). Occupancy factor for K in X site is 0.972(4) for Phase III, 0.972(3) for Phase III′ and 0.9329(13) for Phase IV.

3.1. The $LiK_x(NH_4)_{1-x}SO_4$ mixed crystals

The different phases of the mixed crystals $LiK_x(NH_4)_{1-x}SO_4$ were characterized by single-crystal X-ray diffraction. Atomic coordinates and selected bond lengths and angles are listed in Tables 3 and 4, respectively. Figs. 1 and 2 show the structure down the *c*- and *a*-axis, respectively. Phases III and IV are isostructural to Phases III and IV, respectively, of $LiKSO_4$ [1]. The difference between Phases III and III′ is the rotation of 60° around the *c*-axis of the sulfate ion, which causes Phase III′ to be the enantiomorph of Phase III. The existence of Phase III′ was suggested more than 100 years ago by Traube [15,16]. The crystal structure has now been solved. The identification of a phase whose chirality depends on the preparation had already been observed in $LiNH_4SO_4$ [5]. Klapper et al. [17] studied the twin domains and twin boundaries in $LiKSO_4$, which suggest that Phase IV is a twinned Phase III. We consider that the X-ray intensity measured in a twin crystal is equal to $Iobs[hkl] = x\,I[hkl] + (1-x)\,I[S(hkl)]$, where S is the twin law as, for example, happens in [5,18]. On the other hand if $Iobs(hkl) = I(hkl)$ we consider that the structural model corresponds to a phase [19]. For this reason we consider the existence of a Phase IV which is a disordered phase. However, the disordered phase is at low temperature, which suggests that the disorder is static and is formed by multiple domains of Phase III and III′. This conclusion agrees with the equivalent thermal coefficients obtained. From this result and Table 2 we conclude that two processes lead to the crystallization. The increase of the NH_4^+ concentration diminishes the crystallization rate because the mixture is more soluble in water, which leads to the formation of stable phases and, on the other hand, the NH_4^+ acts as a poisoned site, producing the enantiomorph form of Phase III.

Two different processes were followed in the thermal analysis of $LiK_x(NH_4)_{1-x}SO_4$: a warming process followed by a cooling process in the range 298–950 K, using the ATD; and a cooling process, followed by a warming process in the range 298–150 K, using the

Table 4
Bond lengths (Å) and angles (deg) for $LiK_x(NH_4)_{1-x}SO_4$

	Phase III	Phase III′	Phase IV
S–O(2) (×3)	1.471(9)	1.462(2)	1.453(6)
S–O(1)	1.461(3)	1.465(6)	1.472(4)
K–O(2) (×3)	2.842(4)	2.846(3)	2.841(4)
K–O(2) (×3)	2.958(4)	2.958(3)	2.969(4)
K–O(1) (×3)	2.9817(10)	2.9847(9)	2.9929(13)
Li–O(1)	1.910(12)	1.901(9)	1.917(9)
Li–O(2) (×3)	1.920(4)	1.926(3)	1.919(4)
O(2)–S–O(2) (×3)	110.58(17)	110.65(13)	110.60(14)
O(2)–S–O(1) (×3)	108.34(18)	108.26(14)	108.32(15)
O(1)–Li–O(2) (×3)	104.4(4)	105.0(3)	104.7(3)
O(2)–Li–O(2) (×3)	114.0(3)	113.6(2)	113.8(2)

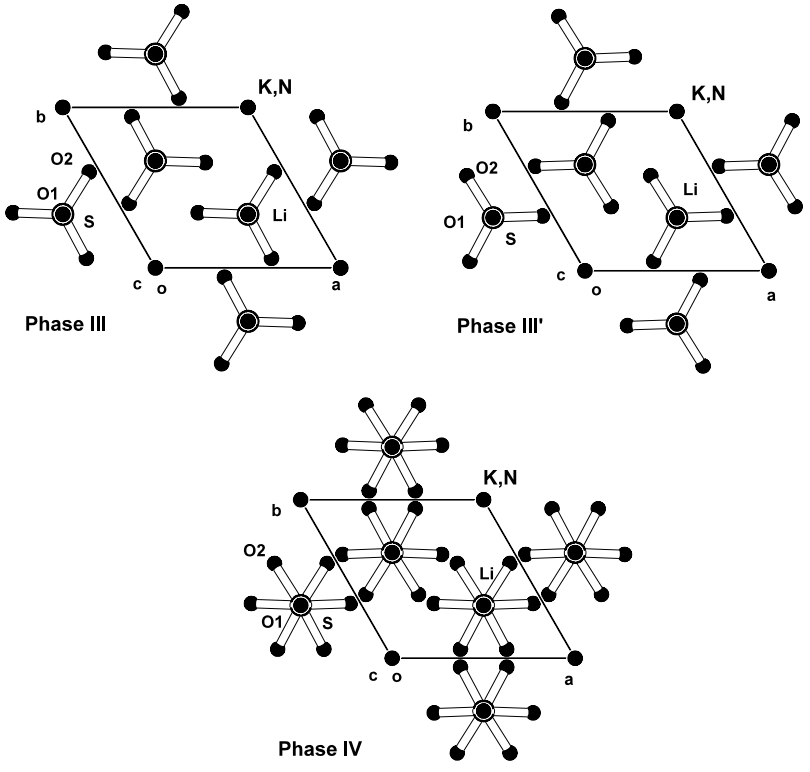

Fig. 1. Projection of the structure of the three obtained phases of $Li[K_{0.94}(NH_4)_{0.06}]SO_4$ down the *c*-axis.

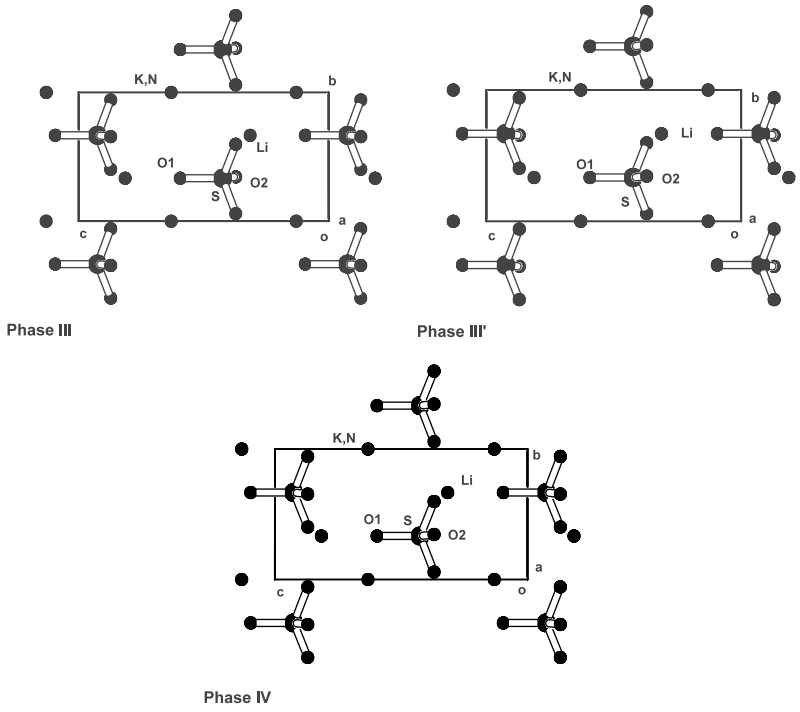

Fig. 2. Projection of the structure of the three obtained phases of $Li[K_{0.94}(NH_4)_{0.06}]SO_4$ down the *a*-axis.

Table 5
Comparison between the phase transition temperature (in K) during the cooling process of $LiKSO_4$ and $LiK_{0.94}(NH_4)_{0.06}SO_4$. Values for $LiKSO_4$ are from [1]

Phase	I	II	III	IV	V	VI
$LiKSO_4$	937	707	226	200	186	T (K)
$LiK_{0.94}(NH_4)_{0.06}SO_4$	923	746	225	212	183	T (K)

DSC. In Table 5, the transition temperatures for $LiKSO_4$ and $LiK_{0.94}(NH_4)_{0.06}SO_4$ are compared. The transition between Phases III and IV was not observed by Raman scattering [9] because the site symmetry is the same in the two phases. The results obtained for the other two-phase transitions at low temperature agree with the results of Freire et al. [9].

From these results we conclude that the metastable Phase IV at room temperature and the new Phase III′ can be obtained by varying the NH_4^+ concentration in the solution, while the same phases that in $LiKSO_4$ are obtained by varying the temperature. The phase transition temperatures are affected by the random presence of the ammonium ion in this disordered system. The transition between the Phase IV and III could be of order–disorder or displacive. However, the disordered phase is at low temperature, so thermodynamic considerations suggest that the Phase IV has multiple domains of $P6_3$ symmetry and the phase transition is displacive. The conclusion that Phase IV has multiple domains agrees with the finding that Phase III′ was obtained by varying the ammonium concentra-

Table 6
Atomic coordinates ($\times 10^4$) and equivalent isotropic displacement parameters ($Å^2 \times 10^3$) for $Li_2KNH_4(SO_4)_2$ at room temperature

	x	y	z	U(eq)
K(1)	3333	−3333	2208(3)	53(1)
K(2)	0	0	2417(2)	40(1)
K(3)	6667	3333	2206(3)	51(1)
S(1)	3342(1)	6(1)	4382(1)	24(1)
S(2)	3278(1)	−1722(1)	307(1)	23(1)
S(3)	5041(1)	1667(1)	313(1)	21(1)
S(4)	1596(1)	−76(1)	297(1)	18(1)
K(1N)	1823(1)	−1502(1)	7314(2)	44(1)
K(2N)	4819(1)	34(1)	7345(2)	40(1)
K(3N)	3354(1)	1438(1)	7406(2)	42(1)
Li(1)	3292(2)	3(2)	456(10)	30(2)
Li(2)	3365(3)	−1719(3)	4106(7)	25(1)
Li(3)	5083(3)	1674(2)	4142(6)	21(1)
Li(4)	1611(2)	−99(3)	4105(6)	22(1)
O(11)	3341(1)	25(2)	2662(4)	46(1)
O(12)	3596(3)	−614(2)	4920(4)	66(1)
O(13)	2490(2)	−196(3)	5012(4)	65(1)
O(14)	4018(2)	831(2)	5030(4)	56(1)
O(21)	2777(2)	−2574(2)	−496(4)	47(1)
O(22)	3001(2)	−1896(2)	1979(3)	44(1)
O(23)	3025(2)	−1095(2)	−230(3)	51(1)
O(24)	4175(2)	−1328(2)	159(4)	57(1)
O(31)	5825(2)	1933(2)	−577(4)	53(1)
O(32)	5230(2)	1572(2)	2010(3)	47(1)
O(33)	4384(2)	815(2)	−246(3)	53(1)
O(34)	4679(2)	2212(2)	200(4)	60(1)
O(41)	1301(2)	593(2)	124(3)	51(1)
O(42)	1436(1)	−349(1)	1954(3)	30(1)
O(43)	2500(2)	289(2)	−71(3)	44(1)
O(44)	1104(2)	−829(2)	−707(4)	62(1)

U(eq) is defined as one-third of the trace of the orthogonalized U_{ij} tensor. Occupancy factor for $K(1N)$, $K(2N)$ and $K(3N)$: $K = 0.333$, $N = 0.667$.

tion in the solution and with the optical observations of $LiKSO_4$ [20].

3.2. The $Li_2KNH_4(SO_4)_2$

$Li_2KNH_4(SO_4)_2$ was characterized by single-crystal X-ray diffraction. Atomic coordinates and selected bond length and angles are listed in Tables 6 and 7, respectively. Projection of the structure are shown in Fig. 3. The crystal structure can be described as a framework of corner-sharing LiO_4 and SO_4 tetrahedra with K^+ and NH_4^+ filling the cavities in the framework. Three symmetrically non-equivalent cavities are occupied by K^+ ions and the other three are randomly occupied by ammonium and potassium ions. The former displays nine-coordination while the latter displays six or seven-coordination. The S(1) sulfate ion acts as the bridge between four lithium ions and five cavities occupied randomly by potassium and ammonium. The remaining sulfate ions in the asymmetric unit act as the bridge between four lithium ions, two potassium ions and four cavities occupied randomly by ammonium and potassium. The structure has the same space group as Phase III of $LiKSO_4$ and a subunit of type of unit cell of

Table 7
Selected bond lengths (Å) and angles (deg)for $Li_2KNH_4(SO_4)_2$

K(1)–O(31) × 3	2.924(4)	K(2)–O(41) × 3	2.844(4)	K(3)–O(21) × 3	2.868(4)
K(1)–O(22) × 3	2.969(3)	K(2)–O(42) × 3	3.005(3)	K(3)–O(32) × 3	2.956(3)
K(1)–O(21) × 3	3.119(5)	K(2)–O(41) × 3	3.102(4)	K(3)–O(31) × 3	3.263(5)
K(1N)–O(44)	2.774(4)	K(2N)–O(12)	2.837(5)	K(3N)–O(22)	2.847(4)
K(1N)–O(34)	2.850(4)	K(2N)–O(33)	2.837(5)	K(3N)–O(14)	2.859(5)
K(1N)–O(23)	2.857(5)	K(2N)–O(24)	2.847(4)	K(3N)–O(43)	2.870(4)
K(1N)–O(13)	2.854(5)	K(2N)–O(32)	2.892(3)	K(3N)–O(42)	2.877(4)
K(1N)–O(43)	3.170(5)	K(2N)–O(14)	3.207(5)	K(3N)–O(34)	3.188(6)
K(1N)–O(11)	3.298(4)	K(2N)–O(24)	3.233(5)	K(3N)–O(13)	3.294(6)
		K(2N)–O(12)	3.359(6)	K(3N)–O(33)	3.314(5)
S(1)–O(11)	1.479(5)	S(2)–O(21)	1.514(3)	S(3)–O(31)	1.469(3)
S(1)–O(12)	1.489(3)	S(2)–O(22)	1.503(4)	S(3)–O(32)	1.528(4)
S(1)–O(13)	1.503(3)	S(2)–O(23)	1.500(3)	S(3)–O(33)	1.485(3)
S(1)–O(14)	1.492(3)	S(2)–O(24)	1.420(3)	S(3)–O(34)	1.441(2)
S(4)–O(41)	1.561(3)	Li(1)–O(43)	1.815(7)	Li(2)–O(31)	1.723(6)
S(4)–O(42)	1.488(4)	Li(1)–O(33)	1.885(5)	Li(2)–O(22)	1.916(8)
S(4)–O(43)	1.467(3)	Li(1)–O(23)	1.896(4)	Li(2)–O(12)	1.964(6)
S(4)–O(44)	1.481(4)	Li(1)–O(11)	1.897(10)	Li(2)–O(34)	2.069(6)
Li(3)–O(21)	1.838(5)	Li(4)–O(41)	1.836(6)		
Li(3)–O(32)	1.874(7)	Li(4)–O(13)	1.863(6)		
Li(3)–O(14)	1.927(5)	Li(4)–O(42)	1.892(7)		
Li(3)–O(24)	1.956(6)	Li(4)–O(44)	1.968(6)		
O(11)–S(1)–O(12)	109.4(2)	O(24)–S(2)–O(23)	107.4(2)		
O(11)–S(1)–O(14)	111.08(19)	O(24)–S(2)–O(22)	111.8(2)		
O(12)–S(1)–O(14)	103.54(19)	O(23)–S(2)–O(22)	104.78(17)		
O(11)–S(1)–O(13)	110.63(19)	O(24)–S(2)–O(21)	115.31(18)		
O(12)–S(1)–O(13)	112.0(2)	O(23)–S(2)–O(21)	112.36(19)		
O(14)–S(1)–O(13)	109.9(2)	O(22)–S(2)–O(21)	104.72(18)		
O(34)–S(3)–O(31)	116.07(19)	O(43)–S(4)–O(44)	108.29(17)		
O(34)–S(3)–O(33)	106.8(2)	O(43)–S(4)–O(42)	110.13(15)		
O(31)–S(3)–O(33)	108.5(2)	O(44)–S(4)–O(42)	108.82(18)		
O(34)–S(3)–O(32)	110.3(2)	O(43)–S(4)–O(41)	111.80(17)		
O(31)–S(3)–O(32)	107.4(2)	O(44)–S(4)–O(41)	112.4(2)		
O(33)–S(3)–O(32)	107.50(16)	O(42)–S(4)–O(41)	105.38(15)		
O(43)–Li(1)–O(33)	111.8(4)	O(31)–Li(2)–O(22)	112.1(3)		
O(43)–Li(1)–O(23)	113.7(3)	O(31)–Li(2)–O(12)	113.9(3)		
O(33)–Li(1)–O(23)	109.8(2)	O(22)–Li(2)–O(12)	113.0(3)		
O(43)–Li(1)–O(11)	106.2(3)	O(31)–Li(2)–O(34)	118.6(3)		
O(33)–Li(1)–O(11)	106.4(3)	O(22)–Li(2)–O(34)	99.9(3)		
O(23)–Li(1)–O(11)	108.5(4)	O(12)–Li(2)–O(34)	98.0(3)		
O(21)–Li(3)–O(32)	107.4(3)	O(41)–Li(4)–O(13)	113.4(4)		
O(21)–Li(3)–O(14)	114.4(2)	O(41)–Li(4)–O(42)	108.9(3)		
O(32)–Li(3)–O(14)	116.4(3)	O(13)–Li(4)–O(42)	115.8(3)		
O(21)–Li(3)–O(24)	115.2(3)	O(41)–Li(4)–O(44)	106.3(2)		
O(32)–Li(3)–O(24)	104.4(2)	O(13)–Li(4)–O(44)	106.2(3)		
O(14)–Li(3)–O(24)	98.5(3)	O(42)–Li(4)–O(44)	105.5(3)		

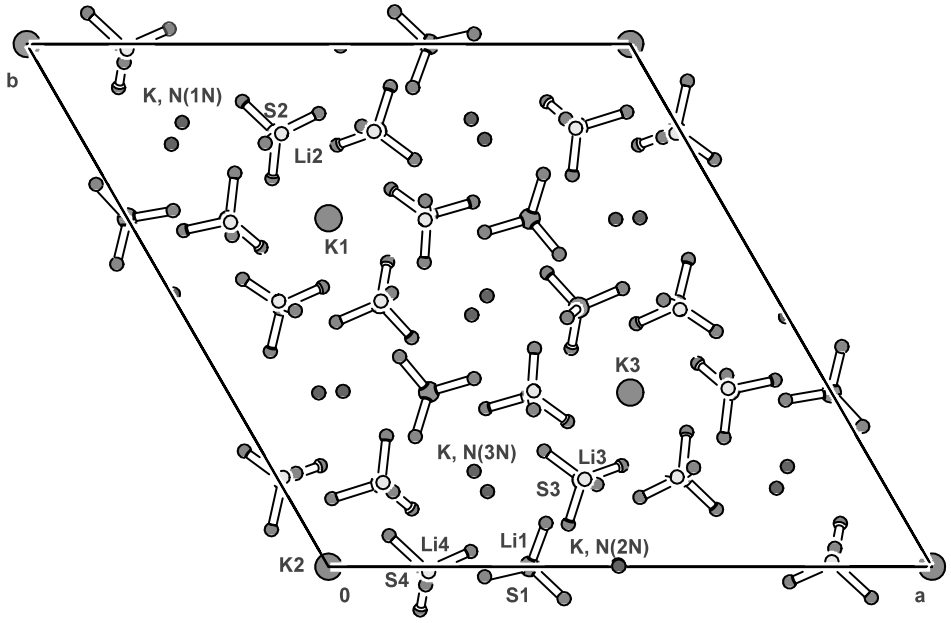

Fig. 3. Projection of the structure of the $Li_2KNH_4(SO_4)_2$ down the c-axis.

$LiKSO_4$ can be defined. The subunit is defined by the vectors $a_{su} = -a/6 - b/3$; $b_{su} = a/3 + b/6$, $c_{su} = c$. The SO_4 ions are not oriented in parallel alignment as in $LiKSO_4$. If the structures at room temperature of $LiKSO_4$ [1], $LiNH_4SO_4$ [5], $LiNaSO_4$ [18,21] and $Li_2KNH_4(SO_4)_2$ are compared, all the unit-cell SO_4 tetrahedra are observed to have the same orientation in $LiKSO_4$, which is parallel to three-fold axes, the relationship between up and down is 3:1 in $Li_2KNH_4(SO_4)_2$, 2:1 in $LiNaSO_4$ and 1:1 in $LiNH_4SO_4$. The total spontaneous polarization for $Li_2KNH_4(SO_4)_2$ has been computed using the observed atomic coordinates and using an ionic model. The value obtained is 9.4×10^{-8} C/cm^2.

Table 8 shows the observed frequencies in Raman scattering of $Li_2KNH_4(SO_4)_2$. The vibration mode assignments in Raman spectra are easily obtained from the vibrational spectra studies for $LiNH_4SO_4$ [5] and $LiKSO_4$ [22–26].

The fitting in ν_2 (SO_4) spectral range was obtained if two peaks were assumed (Fig. 4). Only one mode is observed in this zone in $P6_3$ symmetry, while two modes are observed in $LiNH_4SO_4$ by the site group D_2 symmetry of the SO_4. The shift of ν_2 (SO_4) mode is explained by the different roles of SO_4 in the structure. The fitting in ν_4 (SO_4) zone was obtained using three peaks (Fig. 4), which is similar to the result of Hiraishi et al. [22] for the $LiKSO_4$. The shift of the 1101–1116 ν_3 (SO_4) mode was also observed by Frech et al. [23] in $LiKSO_4$ and Solans et al. [5] in $LiNH_4SO_4$. The remaining weaker peaks in the ν_3 (SO_4) zone are more similar to those observed in $LiNH_4SO_4$. The ν_4 (NH_4)

Table 8
The observed frequencies (cm^{-1}) in Raman scattering of $Li_2KNH_4(SO_4)_2$ which are compared with the Raman modes of $LiNH_4SO_4$ (5) and $LiKSO_4$ (18,19)

	$Li_2KNH_4(SO_4)_2$	$LiNH_4SO_4$(5)	$LiKSO_4$(18)	$LiKSO_4$(19)
t^{SO_4}	46.4(4)	41.14		
t^{SO_4}	58.3(3)			
t^{SO_4}	77.92(9)	76.5		
t^{K}	81.47(7)			
t^{K}	83.16(7)			
t^{NH_4}	197	195.2		
t^{Li}	404	394.6	405	
t^{Li}			411	
$\nu_2^{SO_4}$	458.3(2)	463.9	467	463
$\nu_2^{SO_4}$	474.91(17)	475.1		
$\nu_4^{SO_4}$	625.78(5)	633.2	623	623
$\nu_4^{SO_4}$	641.14(12)	642.3	635	635
$\nu_4^{SO_4}$	657.4(2)		647	
$\nu_1^{SO_4}$	1007.01(3)	1007.83	1012	1013
$\nu_3^{SO_4}$	1100.7(3)	1086.6		1118
$\nu_3^{SO_4}$	1116.4(4)	1104.86	1120	1119
$\nu_3^{SO_4}$		1121.6		
$\nu_3^{SO_4}$	1157.3(3)	1149.9		
$\nu_3^{SO_4}$	1177.3(13)	1175.0		
$\nu_3^{SO_4}$	1252.3(10)	1192.7	1204	
$\nu_3^{SO_4}$	1295.1(4)			
$\nu_4^{NH_4}$		1408.70		
$\nu_4^{NH_4}$	1422.0(5)	1441.5		
$\nu_2^{NH_4}$		1646		
$\nu_2^{NH_4}$	1684.2(11)	1680.55		

Values without e.s.d were not analytically fitted. The given value is the position of peak maximum.

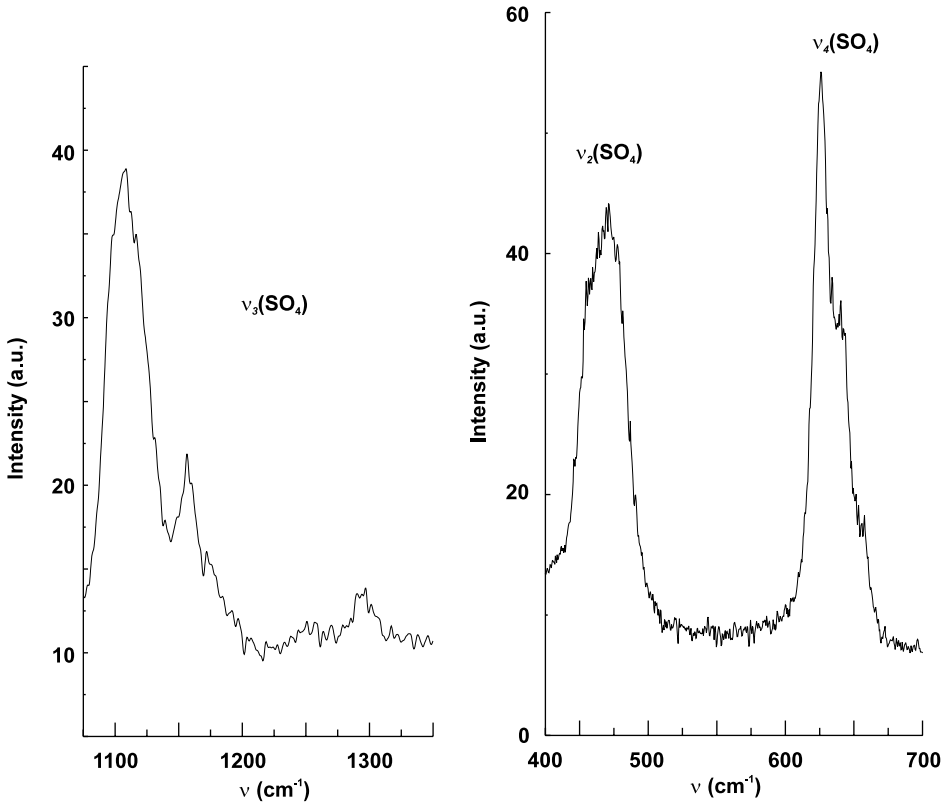

Fig. 4. Selected frequency ranges of Raman scattering of $Li_2KNH_4(SO_4)_2$ at room temperature.

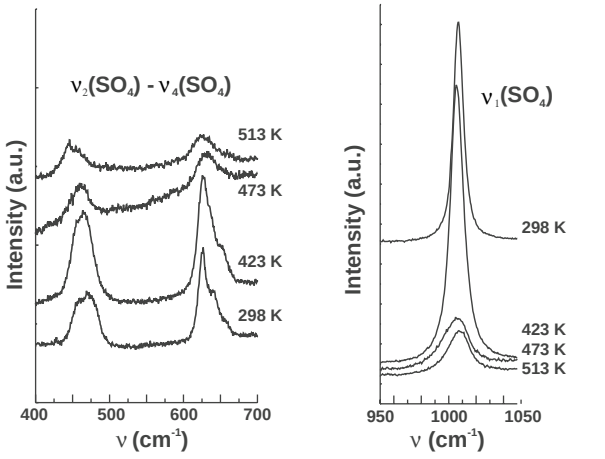

Fig. 5. Selected frequency ranges of Raman scattering of $Li_2KNH_4(SO_4)_2$ at different temperatures. The frequencies were measured in a warming process.

and ν_2 (NH_4) peaks are broader than those observed in $LiNH_4SO_4$, which indicates the disorder in this ion (Fig. 5).

Thermal analyses of $Li_2KNH_4(SO_4)_2$ were made using ATD, TG and powder X-ray diffraction. A phase transition is observed at 471.9 K. The high-temperature Phase is hexagonal, space group $P6_3/mmc$. The cell parameters at 483 K are $a = 10.5569(6)$ and $c = 8.7128(7)$ Å. During cooling (8 h), the transition is not reversible. The cell a parameter of the high-temperature phase is double the value of $LiKSO_4$, so the transition produces ion diffusion. The Raman scattering at different temperatures shows the phase transition of $Li_2KNH_4(SO_4)_2$ and the non-reversibility of the process after 2 h. The frequencies decrease with temperature. This agrees with the results obtained by Frech et al. [23] in $LiKSO_4$. The frequencies tend to overlap and the intensity decreases in inverse proportion to the temperature.

4. Conclusions

The results indicate that two processes lead to crystallization: the increase of the NH_4^+ concentration diminishes the crystallization rate because the mixture is more soluble in water and the NH_4^+ facilitates the formation of the enantiomorph form of Phase III. The use of single-crystal X-ray diffraction has allowed determination of the enantiomorph of the phases obtained. From this, the new Phase III′ was determined and the observation of Phase IV confirms the existence of the same Phase in $LiKSO_4$, determined for the first time in [1]. The framework of corner-sharing LiO_4 and SO_4 tetrahedra is, then, relatively flexible. The phase

transition temperatures for $Li[K_x(NH_4)_{1-x}]SO_4$ $x \geqslant 0.94$ are shown to be affected by the random presence of the ammonium ion in this disordered system.

A new phase $Li_2KNH_4(SO_4)_2$ has been obtained where the SO_4^{2-} ions are not oriented in parallel arrangement as in $LiKSO_4$. Moreover, the relationship between up and down SO_4^{2-} tetrahedra is 3:1. This relationship is higher than the value observed in other similar structures such as $LiNH_4SO_4$ and $LiNaSO_4$ and lower than $LiKSO_4$. The high-temperature Phase is hexagonal, space group $P6_3/mmc$, as in $LiKSO_4$, but the cell a-parameter is double that observed at high-temperature in $LiKSO_4$. The intermediate orthorhombic phase of $LiKSO_4$ is not observed in $Li_2KNH_4(SO_4)_2$. The phase transition is at 471.9 K, showing the high-temperature Phase in greater disorder as indicated by the Raman scattering results.

References

[1] X. Solans, M.T. Calvet, M.L. Martínez-Sarrión, L. Mestres, A. Bakkali, E. Bocanegra, J. Mata, M. Herraiz, J. Solid State Chem. 148 (1999) 316 (and references therein).

[2] M.A. Pimenta, P. Echegut, Y. Luspin, G. Hauret, F. Gervais, P. Abélard, Phys. Rev. B 39 (1989) 3361.

[3] U.A. Leitao, A. Righi, P. Bourson, M.A. Pimenta, Phys. Rev. B 50 (1994) 2754.

[4] C.B. Pinheiro, M.A. Pimenta, G. Chapuis, N.L. Speziali, Acta Crystallogr. B 56 (2000) 607.

[5] X. Solans, J. Mata, M.T. Calvet, M. Font-Bardia, J. Phys.: Condens. Matter 11 (1999) 8995 (and references therein).

[6] V. Lemos, R. Centoducatte, F.E.A. Melo, J. Mendes-Filho, J.E. Moreira, A.R.M. Martins, Phys. Rev. B 37 (1988) 2262.

[7] X. Dongfeng, Z. Siyuan, J. Phys. Chem. Solids 57 (1996) 1321.

[8] X. Dongfeng, Z. Siyuan, Chem. Phys. Lett. 301 (1999) 449.

[9] P.T.C. Freire, W. Paraguassu, A.P. Silva, O. Pilla, A.M.R. Teixeira, J.M. Sasaki, J. Mendes-Filho, I. Guedes, F.E.A. Melo, Solid State Commun. 109 (1999) 507.

[10] R.L. Moreira, P. Bourson, U.A. Leitao, A. Righi, L.C.M. Belo, M.A. Pimenta, Phys. Rev. B 52 (1995) 12591.

[11] G.M. Sheldrick, SHELXS A Computer Program for Crystal Structure Solution, University of Göttingen, 1997.

[12] G.M. Sheldrick, SHELXL A Computer Program for Crystal Structure Determination, University of Göttingen, 1997.

[13] H.D. Flack, Acta Crystallogr. A 39 (1983) 867.

[14] J. Rodríguez-Carvajal, WINPLOTR Laboratoire Léon Brillouin, Paris, France, 2000.

[15] H. Traube, N. Jahrbuch, Mineralogie Bd II (1892) 57.

[16] H. Traube, N. Jahrbuch, Mineralogie Bd I (1894) 171.

[17] H. Klapper, Th. Hahn, S.J. Chung, Acta Crystallogr. B 43 (1987) 147.

[18] J. Mata, X. Solans, M.T. Calvet, J. Molera, M. Font-Bardia, J. Phys.: Condens. Matter 14 (2002) 5211.

[19] W. Clegg, A.J. Blake, R.O. Gould, P. Main, in: Crystal Structure Analysis Principles and Practice, Vol. 144, Oxford Science Publishers, Oxford, 2002.

[20] R. Cach, P.E. Tomaszewski, J. Bornarel, J. Phys. C: Sol. State Phys. 18 (1985) 915.

[21] B. Morosin, D.L. Smith, Acta Crystallogr. 22 (1967) 906.

[22] J. Hirashi, N. Taniguchi, H. Takahashi, J. Chem. Phys. 65 (1976) 3821.

[23] R. Frech, D. Teeters, J. Phys. Chem. 88 (1984) 417.

[24] D. Teeters, R. Frech, Phys. Rev. B 26 (1982) 4132.

[25] S.L. Chaplot, K.R. Rao, A.P. Roy, Phys. Rev. B 29 (1984) 4747.

[26] N. Choudhury, S.L. Chaplot, K.R. Rao, Phys. Rev. B 33 (1986) 8607.